The Mechanics of F-Actin Microenvironments Depend on the Chemistry of Probing Surfaces

James L. McGrath,* John H. Hartwig,† and Scot C. Kuo*

*Department of Biomedical Engineering, Johns Hopkins University, Baltimore Maryland 21205, and †Hematology Division, Brigham and Women's Hospital, Boston Massachusetts 02115 USA

ABSTRACT To understand the microscopic mechanical properties of actin networks, we monitor the motion of embedded particles with controlled surface properties. The highly resolved Brownian motions of these particles reveal the viscoelastic character of the microenvironments around them. In both non-cross-linked and highly cross-linked actin networks, particles that bind F-actin report viscoelastic moduli comparable to those determined by macroscopic rheology experiments. By contrast, particles modified to prevent actin binding have weak microenvironments that are surprisingly insensitive to the introduction of filament cross-links. Even when adjacent in the same cross-linked gel, actin-binding and nonbinding particles report viscoelastic moduli that differ by two orders of magnitude at low frequencies (0.5–1.5 rad/s) but converge at high frequencies ($> 10^4$ rad/s). For all particle chemistries, electron and light microscopies show no F-actin recruitment or depletion, so F-actin microheterogeneities cannot explain the deep penetration ($\sim$100 nm) of nonbinding particles. Instead, we hypothesize that a local depletion of cross-linking around nonbinding particles explains the phenomena. With implications for organelle mobility in cells, our results show that actin binding is required for microenvironments to reflect macroscopic properties, and conversely, releasing actin enhances particle mobility beyond the effects of mere biochemical untethering.

INTRODUCTION

Cytoplasmic actin filaments are organized into networks that serve multiple structural purposes. Microscopically, some actin filaments within the cytoskeleton resist mechanical loads whereas others combine with myosin molecules to generate and transmit contractile tension. Simultaneously, the small pores required for a rigid actin network restrict organelle and granule movement within the cytoplasm (Luby-Phelps et al., 1987). Macroscopically, cell shape and organelle localization are manifestations of multiple microscopic processes that involve actin. Here we use reconstituted actin gels seeded with particles as a model system to explore the relation between the macroscopic and microscopic properties of actin.

Attempts to reconstitute the mechanical properties of cytoplasm have been limited, in part, by the differing techniques required for in vivo and in vitro measurements. The standard for characterizing the mechanical properties of cytoskeletal polymers, mechanical rheometers have yielded a consensus modulus of $\sim$7 dynes/cm^2 for 24 μM F-actin (Xu et al., 1998a), which increases to $\sim$40 dynes/cm^2 with dynamic cross-linking (Wachsstock et al., 1994; Xu et al., 1998b). In contrast, cell moduli estimated by various cell deformations, have yet to reach consensus values. The wide range of estimates (10–50,000 dynes/cm^2; see Yamada et al., 2000 for this survey) can be attributed partly to the fact that different techniques deform different combinations of subcellular domains. Whereas reconstituted F-actin gels appear much weaker than cell cytoplasm, the differing techniques used for cellular and in vitro measurements limits a quantitative resolution of this disparity. A developing approach, laser tracking microrheology (LTM), can be applied to both cells (Yamada et al., 2000) and F-actin gels (this paper; Schnurr et al., 1997) and should facilitate reconstitution efforts.

One of many new passive microrheology techniques (see MacKintosh and Schmidt, 1999 for a review), LTM has unique advantages for cell biology. In these techniques, the viscoelastic mechanical properties of a gel are inferred from the constrained Brownian motions of embedded particles (Mason et al., 1997b; Mason and Weitz, 1995). Unlike traditional rheology, no forces are applied to actively deform materials during measurements. Because probe particles are larger than gel pores, particle motions are determined by network flexibility rather than percolation. As a fast (10^4 Hz) and highly localized ($\sim$5-μm^3 sample volume) assay, LTM is uniquely suited for measurements in dynamic and heterogeneous cell environments (Yamada et al., 2000).

Although particle-based microrheology has been accurate for flexible organic polymers (Mason et al., 1997a,c), results for semi-flexible F-actin (1 mg/ml) are variable and range from $\sim$1 dyne/cm^2 (Schnurr et al., 1997) to $\sim$80 dynes/cm^2 (Gisler and Weitz, 1999). Although issues of actin purification and storage can explain orders-of-magnitude variabilities in F-actin rheology experiments (Tang et al., 1999; Xu et al., 1998a), uncontrolled conditions unique to microrheology may also contribute (Morse, 1998; Maggs, 1998; Crocker et al., 2000).

To develop the foundations of microrheology for cell and reconstitution experiments, we rigorously test the effects of particle surface chemistry on particle motions in F-actin

Received for publication 9 May 2000 and in final form 8 August 2000.

Address reprint requests to Dr. Scot C. Kuo, Department of Biomedical Engineering, School of Medicine, Johns Hopkins University, 720 Rutland Avenue, Ross 724, Baltimore, MD 21205. Tel.: 410-614-2528; Fax: 410-955-0549; E-mail: skuo@bme.jhu.edu.

0006-3495/00/12/3258/09 $2.00

networks. No previous microrheology theories or experiments have considered the effects of actin binding by probe particles. We show that particles used in microrheology experiments are not inert as generally assumed but bind varying amounts of actin. Furthermore, the capacity of particles to bind F-actin correlates with the low-frequency (0.5–1.5 rad/s) moduli of their microenvironments. In gels stiffened by two orders of magnitude through filament cross-links, particles that adsorb actin produce viscoelastic estimates that are in good agreement with macroscopic measurements. By contrast, particles that do not absorb actin fail to sense the mechanical changes introduced by cross-links. To explain these phenomenon we hypothesize that inert particles respond to entropic forces and settle into weakened microenvironments during dynamic gel formation. Our data also confirm reports that F-actin gels are compressible at slow, physiologically relevant frequencies (~1 rad/s) (Schnurr et al., 1997) but become incompressible due to hydrodynamic coupling at higher frequencies (Gisler and Weitz, 1999).

The easy penetration of dense, cross-linked networks by large nonbinding particles has implications for organelle mobility and transport in cytoplasm. Our data illustrates that the density of filaments around organelles in electron micrographs can be a poor predictor of organelle binding state and mobility. Although its mechanism requires further study (see Discussion), deep network penetration by nonbinding particles suggests a phenomenon beyond simple untethering for enhancing organelle mobility in cytoplasm.

MATERIALS AND METHODS

Reagents

Biotinylated (AB07-A) and nonbiotinylated (AKL99-B) rabbit skeletal actin used in particle tracking studies were purchased from Cytoskeleton (Denver, CO). This commercial actin has been purified over a G-150 gel filtration column to minimize CapZ, the primary contaminant in actin preparations (Casella et al., 1995). The purified actin used in actin binding assays was provided as a gift from Susan Craig, Johns Hopkins University.

Avidin (Sigma A-9275), poly-L-lysine (Sigma P-7890), and BSA (Sigma A-7906) were purchased from Sigma Chemical Co. (St. Louis, MO). Streptavidin-conjugated particles (CP01N) were purchased from Bangs Laboratories (Fishers, IN). All other particle chemistries were purchased from Polysciences (Warrington, PA).

Optical instrumentation and data analysis

A detailed description of our instrumentation has been described previously (Mason et al., 1997b; Yamada et al., 2000). Briefly, a low-power laser beam enters the epifluorescence port of an Axiovert 135 inverted microscope (Carl Zeiss, Oberkochen, Germany) and is relayed to a 100× DIC, high-NA objective that focuses the laser at the specimen. The microscope condenser lens and custom lenses relay forward-scattered light to a quadrant photodiode detector mounted above the microscope stage. A particle embedded in a test material is centered in the laser focus by moving a feedback-controlled piezoelectric stage (Queensgate, model NPS-XY-100A, East Meadow, NY). Particle movement deflects the forward-scattered light and creates a photocurrent imbalance across the quadrants of the photodiode detector. This imbalance is analyzed to determine the direction and magnitude of the particle's displacement. Before each experiment prescribed motions of the piezoelectric stage, which includes capacitance position transducers, are used to calibrate difference signals from the quadrant photodiodes.

Our primary data are the trajectories of a particle in two dimensions. Motions along each component direction are analyzed to compute mean square particle displacements (MSDs). The magnitude of the modulus G_d is calculated from x and y direction MSDs using the numerical approximations of Mason et al. (1997b). The modulus represents the combined resistances of viscous and elastic components in the particle's environment and is a function of frequency. The phase angle δ defines the relative contributions of viscous and elastic resistances to particle motion and can be computed from the slope of G_d versus frequency (Booij and Thoone, 1982). For an ideal liquid δ is 90° and for an ideal solid δ is 0°.

Standard preparation of polylysine and BSA-coated particles for microrheology

Carboxylated polystyrene microspheres (2% w/v; 0.914-μm particles) were centrifuged at low speed. After centrifugation, resuspended beads were incubated overnight with 5 mg/ml poly-L-lysine (Brown and Spudich, 1979) or 200 mg/ml BSA in TE (10 mM Tris, 1 mM EDTA) under continuous rotation. Coated particles were washed by five cycles of low-speed centrifugation and resuspension in TE.

Quantification of the F-actin-binding capacity of various particle surface chemistries

Polylysine- and BSA-coated particles were prepared as described above for microrheology experiments except particle densities were tripled (polylysine) or doubled (BSA) to improve signal on protein gels. Particle chemistries shown in Fig. 2 were added to 0.6 mg/ml G-actin in buffer A (2 mM Tris, 0.2 mM $CaCl_2$, 0.5 mM β-mercaptoethanol (BME), 0.5 mM ATP, pH 8.0). The actin in these suspensions was polymerized by addition of 10X buffer B (1.5 M KCl, 0.05 M $MgCl_2$, 1 mM EGTA, 5 mM ATP, 0.1 M Tris, 5 mM BME, pH 7.4). Particles were incubated with F-actin for 5 h at room temperature under continuous rotation. After incubation with F-actin, particles were washed with five cycles of centrifugation and resuspension in 1X buffer B. A small volume was removed from each sample and diluted 100-1000-fold in TE. The particle number in these diluted suspensions was determined by counting particles in a hemacytometer under high magnification. To the remaining particles, Laemmli SDS sample buffer was added to solubilize actin adsorbed to the particle surfaces and the mixture was heated for 2 min at 100°C. Without centrifugation, the bead/protein suspension in sample buffer was loaded directly onto polyacrylamide gels for analysis by SDS-PAGE and Coomassie protein staining. An equal number of particles (6.6×10^8 particles) were loaded in each lane of the protein gels. Protein concentrations were determined by quantitative densitometry against standards in the same gel.

Characterization of BSA adsorption on polystyrene particles

Quantification of BSA adsorption to particles was done in a manner similar to the F-actin adsorption studies above except that larger (3 μm) and fewer ($\sim 4 \times 10^7$ per lane) particles were used. To estimate fractional surface occupancy by BSA, we assumed a circular parking area with radius 3.7 nm for BSA (Meechai et al., 1999). The stability of the BSA coat was studied by diluting coated particles in TE for 1 day or 2 weeks, washing beads, and quantifying the BSA that remained adsorbed on the particles.

As shown in Fig. 1 *B*, high concentrations of BSA (10–40% w/v) are required for maximal coating, and these treatments fell short of completely

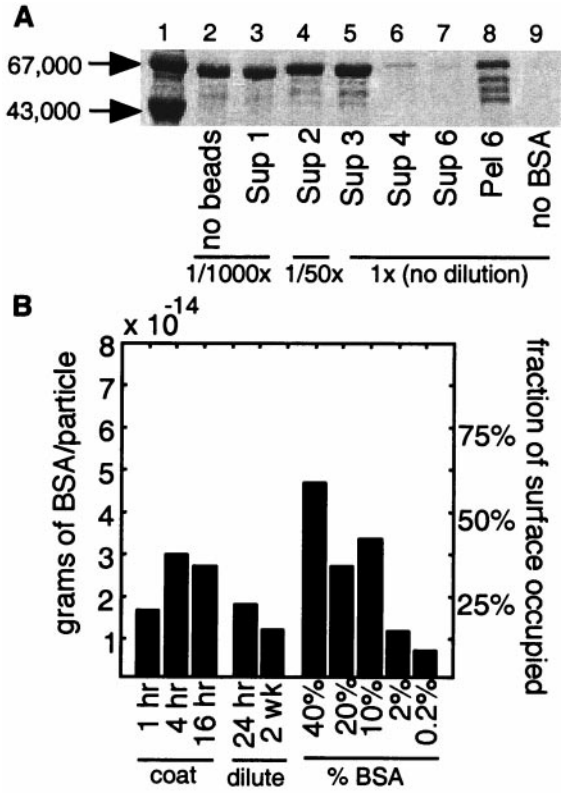

FIGURE 1 Manufacture and stability of BSA-coated particles. (*A*) Construction of BSA-PS beads. Polystyrene particles (3 μm) were incubated with 20% (w/v) BSA overnight. Shown are 2-μl volumes of supernates from successive particle washes (*lanes 3–7*) and particle-adsorbed protein (*lane 8*). BSA adsorbed to particle surfaces appears in multiple bands. Controls without particles (*lane 2*) or without 20% BSA (*lane 9*) ensure the additional protein bands are not contaminants from components of the incubation mixture. To avoid signal saturation, samples were diluted as indicated. (*B*) Kinetics and stability of BSA coating. Four aspects of the coating process are characterized: 1) BSA coats particles in ~4 h, but 2) slowly comes off after washing and dilution into water; 3) a coating solution of 10% BSA or higher is required for maximal coating, and 4) maximal coating never exceeds 50% of the particle surface.

covering particle surfaces. Maximal coating requires at least a 4-h incubation of particles with BSA and is stable for about a day upon washing and dilution into BSA-free buffers. These results led to our standard BSA coating protocol detailed above.

Microrheology experiments in non-cross-linked gels

Before mixing with actin, most particle chemistries were diluted to 0.02% w/v in buffer A. Exceptions were streptavidin and polylysine particle chemistries, which were aggregated. These chemistries were diluted to 0.2% w/v in buffer A to increase the number of monomeric particles available for tracking. A 50-μl sample was prepared that contained 33 μl of 1.5 mg/ml actin (purchased from Cytoskeleton, Boulder, CO), 10 μl of buffer A, 2 μl of particles, and polymerization initiated with 5 μl of 10X buffer B. Polymerizing actin was immediately loaded between a glass slide and coverslip, which were separated by Scotch double-stick tape (~75 μm thick). Beads of silicone vacuum grease prevented the actin/bead solution from touching the double-stick tape. Slides were sealed by streaking molten VALAP (1:1:1 Vaseline, lanolin, and paraffin) along the edges of the coverslip. To reach mechanical equilibrium, slides were incubated for 5 h at room temperature before microrheology measurements. All particles used in these experiments were between 0.91 and 1.0 μm.

Experiments in cross-linked gels

Microrheology measurements in avidin cross-linked networks were done in 0.67 mg/ml to permit comparison with the macroscopic rheometery experiments of Wachsstock et al. (1994). A 50-μl volume was prepared with 21 μl of 1.5 mg/ml actin, 13.67 μl of buffer A, 3.33 μl of 1.0 mg/ml biotinylated actin, and 2 μl of a bead mixture. For direct comparisons, the bead mixture always included BSA-coated fluorescent particles (BSA-PS) and either carboxylated polystyrene (COO-PS) or polylysine-coated polystyrene (PLY-PS) particles. Beads were incubated with monomeric actin for 10 min before the addition of 5 μl of 10X polymerization buffer. Polymerization proceeded for 10 min at 37°C before the introduction of 5 μl of avidin to reach final concentrations of 0.3 μM, 0.1 μM, 0.03 μM, or 0 μM. Solutions were briefly vortexed after the introduction of avidin. This preparation protocol was reproducible in creating homogeneous and strong gels. Alternative approaches in which avidin was added 60 min after polymerization (no vortexing) or before polymerization (vortexing) occasionally produced weaker or inhomogeneous gels. After the addition of polymerization buffer, samples were immediately loaded into slide chambers as described above and allowed to reach mechanical equilibrium for a minimum of 5 h. Final avidin concentrations correspond to actin:avidin ratios of 50:1, 150:1, and 500:1 or filament length per avidin values of 0.13 μm, 0.4 μm, and 1.3 μm, respectively. In a dilute suspension of avidin without filaments, the three-dimensional separation between avidin molecules would be 0.10, 0.14, and 0.21 μm, respectively (Chandrasekhar, 1943). All particles used in these experiments were 0.91 μm.

Electron microscopy

The structure of actin near particles was studied in the electron microscope in unfixed, rapidly frozen samples. G-actin was mixed with particles (0.914 μm) in 0.1 mM EGTA, 0.5 mM ATP, 0.01 M Tris, 0.5 mM BME, pH 7.4, and polymerized by adding final concentrations of KCl and $MgCl_2$ of 10 mM and 1 mM, respectively. The final actin concentration was 1 mg/ml. Immediately after adding salts, 5-μl volumes were placed on the surface of 3-mm square coverslips and incubated overnight at 4°C in a humidified chamber. Samples were rapidly frozen by impact with a liquid-helium-cooled copper block. The frozen samples were fractured using a liquid-nitrogen-cooled knife at −120°C, the newly exposed surface was etched for 30 min at −90°C, and the sample was then coated with 1.4 nm of tantalum-tungsten with rotation and 3.0 nm of carbon without rotation (Cressington Scientific Instruments, Watford, UK). The metal replicas were separated from the coverslip, transferred to copper grids, and examined and photographed at 100 kV in a JEOL-1200 EX electron microscope. We confirmed that the disparity in microrheology reported by actin-binding and inert particles persisted in the low-salt buffer used in samples prepared for EM (data not shown).

RESULTS

Effect of surface chemistry on actin adsorption to polystyrene particles

To explore the effect of filament binding, recruiting, and exclusion by particle surfaces, we sought particle chemistries that would amplify these effects if they exist. To amplify actin binding, we chose polylysine-coated polystyrene particles (PLY-PS), which directly nucleate actin fila-

ments from their surfaces (Brown and Spudich, 1979). To generate particles that would not absorb actin, we blocked particle-actin interactions by preadsorbing BSA to the surface of carboxylated polystyrene particles. We also examined actin binding by bare carboxylated polystyrene particles (COO-PS) and silica particles, both of which have been used in LTM applications in F-actin (Schnurr et al., 1997; Palmer et al., 1999), and amino-conjugated and plain polystyrene particles to examine the role of surface charge. As shown in Fig. 2, with the exception of BSA-PS particles prepared by a standard protocol (see Materials and Methods), all particles adsorbed significant amounts of actin. By quantitative densitometry, BSA-PS particles bind fewer than 10 molecules of actin on average.

Microrheology measurements depend on the choice of probe surface chemistry

For non-cross-linked F-actin gels, surface chemistry is important in determining moduli and phase angles measured in LTM experiments (Fig. 3). At all frequencies (Fig. 3 *A*) BSA-PS particles report the lowest moduli among the chemistries studied and PLY-PS particles report the highest moduli. Because BSA-PS- and streptavidin-conjugated (STA) particles in nonbiotinylated F-actin appear comparable over all frequencies, they are likely equivalently inert. At low frequencies (0.1–1 rad/s) in Fig. 3 *B*, BSA-PS particles report the smallest phase angle of any chemistry, but at the highest frequencies (100–1000 rad/s) these same particles report the largest phase angle of any particle chemistry. Because phase angle indicates the relative contribution of viscous and elastic resistances to particle motion, BSA-PS particles experience both a low-frequency regime in which elastic resistances dominate viscous resistances and a high-frequency regime where viscous resistances dominate elastic resistances. The other particle chemistries show similar, but more subtle, tendencies in phase angle behavior.

Most relevant for cell biology, low-frequency moduli (0.5–1.5 rad/s) for various particles are compared in Fig. 3 *C*. Behaviors appear to separate into three classes. The highest moduli are reported by PLY-PS particles (~1.75-fold higher than COO-PS). The weakest moduli are reported by BSA-PS particles and STA particles in a nonbiotinylated gel (~4-fold lower than COO-PS). The remaining chemistries agree with COO-PS particles to within 0.75–1.25-fold. Derivatization of polystyrene with negative (COO^-) or positive groups (NH_3^+) has only a small effect on moduli. Adding biotinylated sites to filaments in gels containing STA particles increases low-frequency moduli from BSA-PS to COO-PS levels, indicating that filament binding by particles directly enhances moduli.

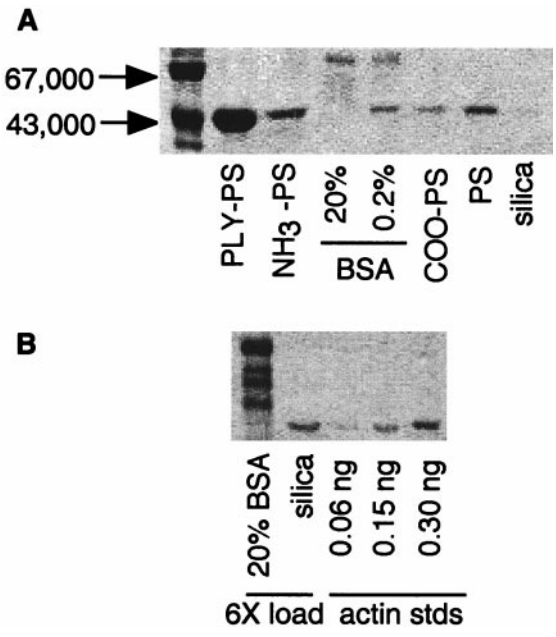

FIGURE 2 Actin binding capacity of particles. (*A*) Actin binding by various particles. At a particle density of ~6×10^8 particles per lane, polylysine-coated (PLY-PS) carboxylated (COO-PS), amino-conjugated (NH_3-PS), and bare polystyrene (Bare-PS) particles bind detectable amounts of actin whereas BSA-coated (BSA-PS) and silica particles do not. (*B*) Actin-binding capacity of silica and BSA-PS particles. With sixfold more particles (4.2×10^9 particles per lane) than *A*, actin adsorption is detected on silica particles but not on BSA-PS particles. Particles were incubated with 0.63 mg/ml F-actin for 4 h and washed extensively before a final suspension in Laemmli SDS sample buffer to solubilize adsorbed protein. The fragments of BSA seen in lane 1 are also seen in experiments without actin (Fig. 1 *A, lane 8*).

Low-frequency moduli correlate with the actin-binding capacity of particles

In comparing apparent moduli with actin-binding capacity, a positive correlation is clear (Fig. 4). By this correlation, the three tiers of weak, intermediate, and high moduli revealed in Fig. 3 *C* appear to correspond to near zero, moderate, and high levels of actin binding, respectively. All particles in Fig. 4 are derivatives of Bare-PS except silica.

Actin binding by particles is required for mechanical sensitivity to gel cross-linking

To explore a larger range of F-actin network mechanics, we examined gels cross-linked with avidin/biotin. We chose avidin/biotin cross-linking because multiple mechanical rheometry experiments report consistent values for these gels (Wachsstock et al., 1994; Xu et al., 1998b; Janmey et al., 1990). Matching the network conditions of Wachsstock et al. (1994) we compared three surface chemistries as avidin concentrations varied in partially biotinylated, 15 μM actin (Fig. 5 *A*). At the two extremes zero and maximal cross-linking (0.3 μM avidin), COO-PS and PLY-PS report

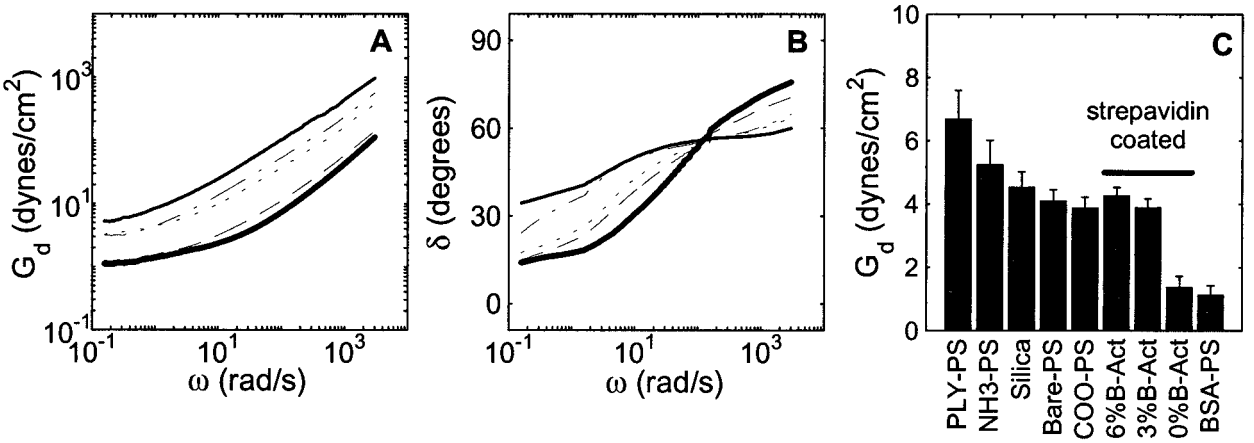

FIGURE 3 Microrheology with various particle chemistries. (*A*) Spectra of micromechanical moduli depend on particle surface chemistry. In order from highest to lowest moduli the chemistries shown are PLY-PS (*thin solid line*), COO-PS (*dash-dotted line*), streptavidin-conjugated (STA) particles in 6% biotinylated actin (*dotted line*), STA particles with 0% biotinylated actin (*dashed line*), and BSA-PS (*thick solid line*) particles. (*B*) Micromechanical spectra of phase angles vary with surface chemistry. BSA-PS-coated particles sense a more solid environment at low frequencies and a more liquid-like environment at high frequencies than polylysine. As with moduli, PLY-PS and BSA-PS particles define extreme behaviors. (*C*) Low-frequency (0.5–1.5 rad/s) moduli for various particles. Most chemistries report a stiffness intermediate to BSA-PS and PLY-PS. The introduction of biotinylated F-actin increases moduli for STA particles from BSA-PS to COO-PS levels. This suggests that filament binding may explain the differences between these chemistries. Error bars span the 95% confidence intervals on the means. Statistics for PLY-PS, COO-PS, and BSA-PS particles were determined from 17–25 particles distributed over four similarly prepared gels. The difference between moduli for these particles are statistically significant ($P_{\text{PLY-PS/COO-PS}} < 0.001$; $P_{\text{COO-PS/BSA-PS}} < 0.001$). Statistics on the remaining chemistries are determined using 6–9 particles distributed in single gels. Data for each particle were determined from the average of three sequential tracking experiments.

moduli that agree well with mechanical rheometry. At intermediate levels of cross-linking PLY-PS particles reasonably mimic macroscopic behavior, although COO-PS particles significantly depart from macroscopic values. Although assembled and measured in the same gels as actin-binding particles, moduli for nonbinding BSA-PS are remarkably insensitive to gel cross-linking.

As shown in Fig. 5 *B*, the behaviors of actin-binding and nonbinding particles depend on the frequency of deformation. Qualitatively, both chemistries sense an elastic environment at low frequency and a more viscous environment at higher frequencies. However, the transition between these behaviors occurs at a lower frequency for inert particles ($\omega \approx 5$ rad/s) than actin binding particles ($\omega \approx 500$ rad/s). As discussed later (see Discussion) the convergence at high frequency for actin-binding and nonbinding behavior is explained by viscous coupling between solvent and filaments.

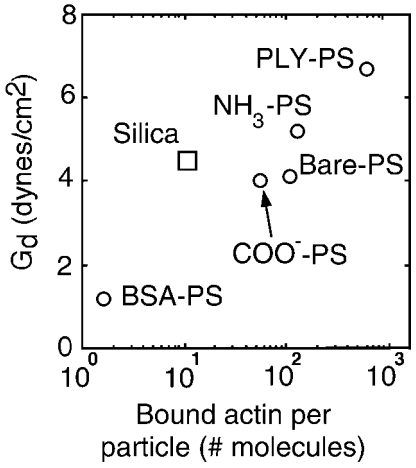

FIGURE 4 Correlation of low-frequency moduli with actin-binding capacity. The actin-binding capacity (Fig. 2) correlates positively with moduli (Fig. 3). We conservatively estimate that BSA-PS particles adsorb less than 10 molecules of actin on average.

To ensure that BSA does not create a mechanically interfering layer on the surface of polystyrene particles, we compared the motion of BSA-PS and COO-PS in polyethylene oxide (PEO). The BSA surface layer might interfere with LTM if it was both thick and softer than F-actin. In this case, LTM measurements would reveal the mechanics of the BSA layer rather than F-actin. To address this, the motions of BSA-coated and uncoated particles were compared with 3% polyethylene oxide, which has a modulus comparable with cross-linked F-actin. At all frequencies in Fig. 5 *B*, BSA-coated and uncoated particles behave identically in this material. This and other evidence (see Discussion) support a conclusion that BSA layers alone do not interfere with LTM in F-actin.

Gels are homogeneous on large length scales

One possible explanation for the divergent behavior of actin-binding and nonbinding particles is that they partition into different domains of heterogeneous gels. However, when actin-binding and nonbinding particles are co-local-

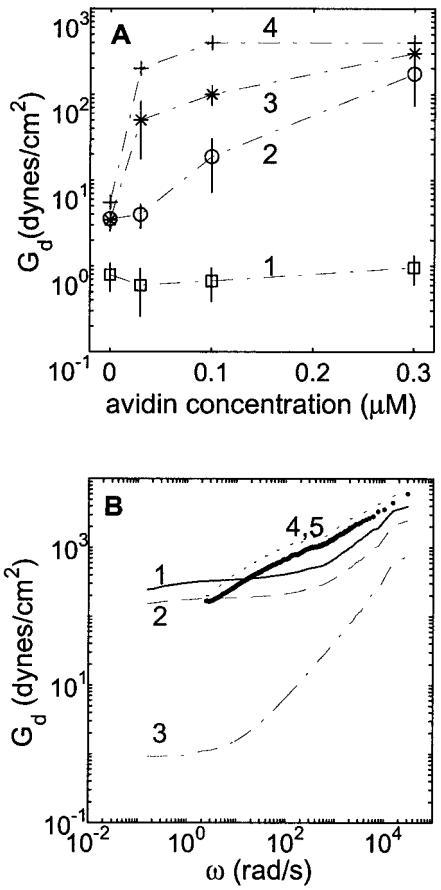

FIGURE 5 Probe sensitivity to network cross-linking. (*A*) Low-frequency (0.5–1.5 rad/s) behavior of particles with increasing cross-linking. BSA-PS particles (*1*, □) are insensitive to the introduction of network cross-links. In non-cross-linked and the most strongly cross-linked gels COO-PS (*2*, ○) and PLY-PS (*3*, *) moduli agree well with published mechanical rheometery values (*4*, +) (Wachsstock et al.; 1994. Error bars are 95% confidence intervals on the means. Statistics are computed from 9–15 particles distributed over three to five similarly prepared gels. Values for individual particles were determined from the average of three sequential tracking experiments. (*B*) Mechanical spectra for different particle chemistries in cross-linked gels. In a highly cross-linked gel (0.3 μM avidin), actin-binding chemistries (PLY-PS, *1* and *thin solid line*; COO-PS, *2* and *dashed line*) diverge 100-fold from BSA-PS particles (*3* and *dash-dotted line*) at low frequencies but converge at high frequencies. In polyethylene oxide (PEO) of comparable modulus to cross-linked F-actin (3% PEO), COO-PS (*4* and *dotted line*) and BSA-PS (*5* and *thick solid line*) behave identically. This ensures that BSA does not make a mechanically compliant layer between the particle and F-actin (see Discussion). All experiments were done in 2/3 mg/ml actin to match the conditions of Wachsstock et al., 1994.

ized in a highly cross-linked gel, they still exhibit an order-of-magnitude difference in the amplitude of their Brownian motions (Fig. 6). In the example shown, ~1-μm BSA-PS and COO-PS particles are separated by 2 μm (Fig. 6 *A*). The mechanical spectra for the particles in this example (Fig. 6, *C* and *D*) match the spectra of Fig. 5 B where multiple particles are averaged in multiple gels. Other arguments also suggest a lack of large-scale heterogeneities. First, particles of a single chemistry appear to distribute uniformly in the same gel (J. L. McGrath, personal observation). Second, the variability of moduli obtained from a single particle type in different places within gels is small (see error bars in Fig. 5 *A*). Collectively, these observations suggest that if discontinuities do occur in these F-actin gels, they occur on dimensions smaller than a particle diameter (<1 μm).

Particles do not exclude or recruit filaments near their surface

We looked for heterogeneity in filament density around particles by high-resolution electron microscopy of particles in unfixed, rapidly frozen F-actin samples (non-cross-linked; 1 mg/ml). In the electron micrographs shown in Fig. 7, the density of filaments near the particle surfaces appears similar to the bulk filament density. Furthermore, the recruitment of filaments to the surfaces of actin-binding particles does not increase local filament density above the apparent bulk concentration (Fig. 7, A and *B*), although there is subtle reorientation of filaments near particle surfaces. We note that the average amplitude of particle motions (overlay in Fig. 7 *C* for BSA-PS particles) is much larger than the apparent width of filaments and pores in these micrographs.

DISCUSSION

The constrained Brownian motions measured by laser-tracking microrheology (LTM) are a direct assessment of the microscopic mechanical environment around particles. In cells, the micromechanical properties of cytoplasmic networks affect the mobility of organelles and granules. If microscopic mechanics reflect macroscopic mechanics, then LTM also provides unique abilities for measuring the macroscopic mechanics of dynamic and heterogeneous cells. Because F-actin is a semiflexible polymer with significant persistence length, microscale and macroscale rheology may not agree for F-actin networks as they do for flexible polymer solutions (Maggs, 1998). Hence, to realize the full promise of LTM for cell biology, the relationship between the microscale behavior revealed by LTM and macroscopic moduli must be understood.

Here we demonstrate the important role of particle surface chemistry in F-actin microrheology. For non-cross-linked actin networks, we find a positive correlation between the capacity of a particle to adsorb F-actin and the mechanical strength of its microenvironment. The unrecognized role of actin adsorption to particle surfaces may partially account for the variability in previous F-actin microrheology experiments (Schnurr et al., 1997; Gisler and Weitz, 1999; Palmer et al., 1999). The disparity between actin-binding and inert (nonbinding) chemistries increases

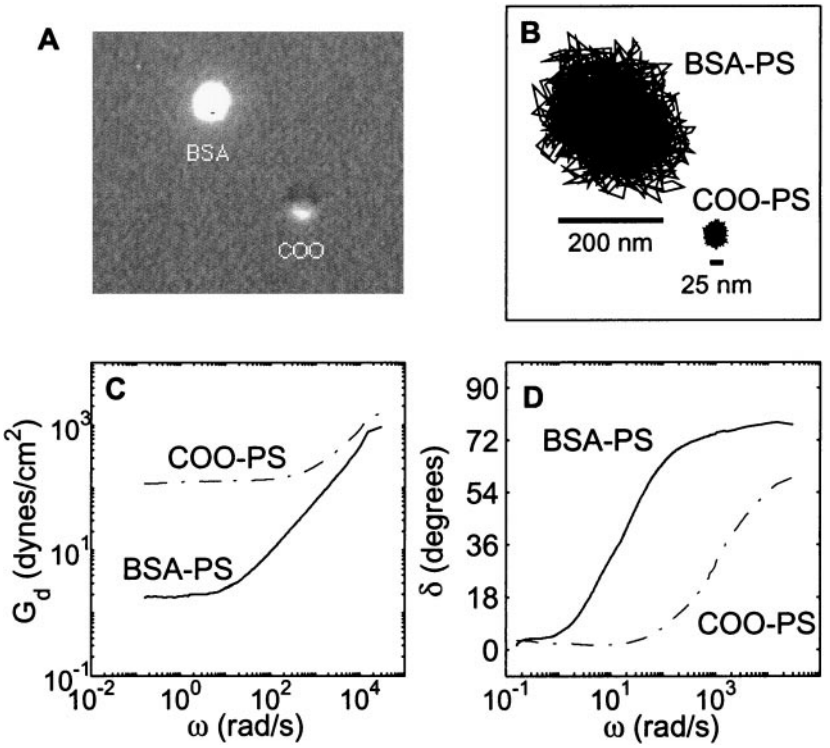

FIGURE 6 Different microenvironments for nearby particles. (*A*) Comparison of adjacent binding and nonbinding particles. A fluorescent inert (BSA-PS) particle resides only ~2 μm from a nonfluorescent actin-binding (COO-PS) particle in a heavily cross-linked (0.3 μM avidin) gel. Both particles are ~1 μm despite an apparent size difference resulting from simultaneous fluorescence and DIC imaging. (*B*) Trajectories of BSA-PS and COO-PS particles during 2.2 s of tracking at 30 kHz. Particles exhibit an order-of-magnitude difference in the amplitude of their motions. (*C*) Micromechanical spectra of moduli. Particle motions reveal large differences in the mechanical modulus of microenvironments at low frequency, but small differences at high frequency. (*D*) Phase angle spectra. The microenvironments of both particles are solid-like at low frequency (phase angle $\delta \approx 0$) and liquid-like at high frequency ($\delta > 45$); however, the transition occurs at a lower frequency for BSA-PS particle.

when gels are stiffened through filament cross-linking. As a group, actin-binding particle chemistries give good agreement with consensus values from macroscopic rheometry for both non-cross-linked and highly cross-linked F-actin gels. Small differences between specific actin-binding particles appear at intermediate cross-linking levels, but these differences disappear in gels of more physiological strengths. Remarkably, inert particles maintain their ability to penetrate actin networks despite the presence of cross-links that enhance macroscopic moduli 100-fold. Therefore, actin binding is an essential requirement for probes used to measure macroscopic moduli.

The vastly different microenvironments sensed by actin-binding and nonbinding particles are not due to the construction of inert particle surfaces. The protein coat on BSA-PS particles could interfere with microrheology assays if the layer were both compliant and overly thick. In this case, the moduli measured would reflect the mechanics of the protein coat rather than those of the embedding gel. Several lines of evidence suggest that BSA does not form an interfering barrier on polystyrene particles. First, commercial streptavidin-conjugated particles suspended in nonbiotinylated F-actin behave identically to BSA-coated particles (Fig. 3 *A*). Because these different proteins are coupled to particles differently, it is unlikely that they would form mechanically similar layers. Second, the amount of BSA on inert particles is much less than required to form a complete protein monolayer (Fig. 1 *B*). If BSA molecules remain

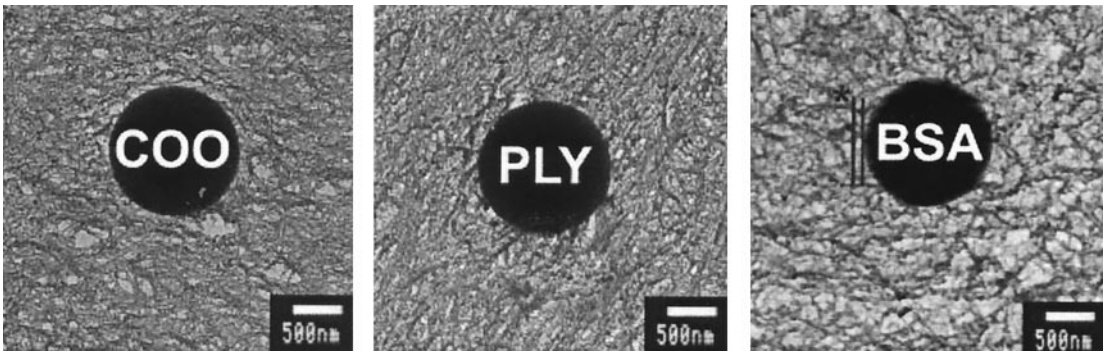

FIGURE 7 Electron micrographs of particle/network interfaces. COO-PS, PLY-PS, and BSA-PS particles cause little disturbance to an non-cross-linked 1 mg/ml actin gel. The average amplitude of BSA-PS particle motions (~100 nm) are shown in the leftmost panel. These displacements are ~10% of the particle diameter and much larger than the apparent average width of filaments and pores in this image.

monomers, the coat would extend only ~7 nm (Meechai et al., 1999) from the particle surface, which is an order of magnitude smaller than BSA-PS particle motions (~100 nm). Third, a BSA layer comparable in size to particle motions is not observed in electron micrographs of the particle/gel interface (Fig. 7). Finally, in PEO solutions that match actin moduli, BSA-coated and noncoated particles have identical behavior (Fig. 5 *B*). Collectively, these results demonstrate that BSA molecules do not assemble into compliant aggregate layers that interfere with LTM measurements.

The different microenvironments are not due to filament recruitment or exclusion by particles. When embedded in a gel formed from rigid and uniformly long filaments, an inert particle will locally deplete filaments by sterically excluding all filaments at its surface and ~70% of filaments at 1/2 radius from its surface (Morse, 1998). Electron micrographs (Fig. 7) show no such filament depletion zone around nonbinding particles, suggesting that reconstituted F-actin is not sufficiently rigid or uniformly long to match this calculation. Furthermore, F-actin is not recruited by actin-binding particles (Fig. 7). We conclude that the uniformity of actin density regardless of particle chemistries precludes inferring micromechanics from actin density alone.

The different microenvironments sensed by actin-binding and nonbinding particles may instead arise from microscopic cross-linking heterogeneities. Because the highest avidin concentrations (0.3 μM avidin) should produce cross-links separated by ~100 nm on average, gels will contain many regions that are larger than inert particle motions and devoid of cross-links. Thermodynamically, the migration of nonbinding particles to these weakened microdomains is entropically favorable because it maximizes particle motions. Soft microenvironments could be selected during the process of gelation as inert particles migrate through the forming gel. Additionally, soft pockets could form around inert particles because their large motions inhibit cross-link formation. In contrast, actin-binding particles should be prevented from migrating during the formation of cross-links and therefore be more representative of the bulk gel.

Whereas actin-binding and nonbinding particles sense different F-actin microenvironments at low frequency, solvent and filament coupling mandates that they sense the same viscoelastic moduli at high frequencies. This convergent behavior is most obvious with strong cross-linking (Figs. 5 *B* and 6 *C*6) and is best explained by considering that F-actin solutions are composed of a compressible network of filaments immersed in an incompressible solvent. Compressibility arises at low frequencies because fluid can be expelled from regions of the network as a particle moves. As the frequency of excitation increases, however, the viscous drag imparted on filaments by the solvent flowing through filament pores also increases. Eventually, at high enough frequencies, the relative motion of solvent and filament phases cannot occur and these phases become hydrodynamically coupled (DeGennes, 1976). Our results agree with previous findings that strong hydrodynamic coupling occurs at frequencies greater than 10^4 rad/s (Gisler and Weitz, 1999).

The lack of correlation between micromechanics and actin density has implications for cell biology, particularly for intracellular organelle transport through dense networks. By using controlled particle surfaces in dense actin, we have shown that actin density appears uniform around all particle chemistries. Clearly, microfilament density alone can be a poor predictor of an organelle's binding state, mobility, or strength of its microenvironment. Furthermore, the mechanisms that promote the easy penetration of inert particles in actin networks should also promote the penetration of organelles into dense cytoplasm.

For example, our results may help explain the motions of secretory granules in chromaffin cells of the adrenal medulla. In these cells, large granules (300 nm) exhibit large Brownian motions (70 nm; Steyer and Almers, 1999) despite being embedded in a dense cortical actin network (Nakata and Hirokawa, 1992). By comparison, Brownian motions are sevenfold smaller for comparably sized lipid droplets in lamellae of Cos7 cells (Yamada et al., 2000). Unless Cos7 lamellae are ~50-fold stiffer than the cortex of chromaffin cells, chromaffin granules are unusually mobile. Consistent with our observations of reconstituted particles, granule surfaces may resist significant actin adsorption as a mechanism to promote penetration of the cortical network.

In summary, we have found that the measurement of F-actin microviscoelasticity depends on the chemistry of the surfaces used as probes. The microenvironments around actin-binding particles have macroscopic viscoelastic properties, particularly at high levels of cross-linking. In contrast, microenvironments around particles that do not bind actin are unusually soft, regardless of cross-links in the network. Nonbinding particles may entropically migrate into weaker domains of these gels and may directly interfere with cross-link formation in their microenvironment. If organelles resemble inert particles, then these phenomena have implications for organelle distribution and transport in cells. Our data also show that differences in microenvironments appear at low frequencies, but disappear at higher frequencies ($>10^4$ rad/s) where solvent/filament coupling resists compressibility. Clearly, LTM provides more than the capacity for measuring macroscopic moduli in microscopic volumes; LTM provides novel data on F-actin microenvironments unavailable to traditional techniques but relevant to cell physiology.

We thank Soichiro Yamada and Dan Ennis for numerous interactions that have added significantly to our understanding of LTM and microrheology and Jim Harden for helpful discussions and comments on this manuscript. We thank Susan Craig and her laboratory for supplying the actin used in our binding studies. We are grateful to Sarah Chalos for her assistance in processing EMs.

S.C.K. was supported by the National Science Foundation and The Whitaker Foundation. J.L.M. is a Whitaker/Johns Hopkins Biomedical Engineering Distinguished Postdoctoral Fellow. J.H.H. was supported by National Institutes of Health grant HL56252.

REFERENCES

Booij, H. C., and G. P. J. M. Thoone. 1982. Generalization of Kramers-Kronig transforms and some approximations of relations between viscoelastic quantities. *Rheol. Acta.* 21:15–24.

Brown, S. S., and J. A. Spudich. 1979. Nucleation of polar actin filament assembly by a positively charged surface. *J. Cell Biol.* 80:499–504.

Casella, J. F., E. A. Barron-Cassela, and M. A. Torres. 1995. Quantitation of Cap Z in conventional actin preparations and methods of further purification of actin. *Cell Motil. Cytoskel.* 30:164–170.

Chandrasekhar, S. 1943. Reviews of Modern Physics. Dover, New York.

Crocker, J. C., M. T. Valentine, E. R. Weeks, T. Gisler, P. D. Kaplan, A. G. Yodh, and D. A. Weitz. 2000. Two-point microrheology of inhomogeneous soft materials. *Phys. Rev. Lett.* 85:888–891.

DeGennes, P. G. 1976. Dynamics of entangled polymer solutions. II. Inclusion of hydrodynamic interactions. *Macromolecules.* 9:594–598.

Gisler, T., and D. A. Weitz. 1999. Scaling of the microrheology of semidilute F-actin solutions. *Phys. Rev. Lett.* 82:1606–1610.

Janmey, P. A., S. Hvidt, J. Lamp, and T. P. Stossel. 1990. Resemblance of actin-binding protein/actin gels to covalently crosslinked networks. *Nature.* 345:89–92.

Luby-Phelps, K., P. E. Castle, D. Taylor, and F. Lanni. 1987. Hindered diffusion of inert tracer particles in the cytoplasm of mouse 3T3 cells. *Proc. Natl. Acad. Sci. U.S.A.* 84:4910–4913.

MacKintosh, F. C., and C. F. Schmidt. 1999. Microrheology. *Curr. Opin. Colloid Interface Sci.* 4:300–307.

Maggs, A. C. 1998. Micro-bead mechanics with actin filaments. *Phys. Rev. E.* 57:2091–2094.

Mason, T. G., A. Dhople, and D. Wirtz. 1997a. Concentrated DNA rheology and microrheology. *Mat. Res. Soc. Symp. Proc.* 463:153–158.

Mason, T. G., K. Ganesan, J. H. van Zanten, D. Wirtz, and S. C. Kuo. 1997b. Particle tracking microrehology of complex fluids. *Phys. Rev. Lett.* 79:3282–3285.

Mason, T. G., H. Gang, and D. A. Weitz. 1997c. Diffusing-wave-spectroscopy measurements of viscoelasticity of complex fluids. *J. Opt. Soc. Am.* 14:139–149.

Mason, T. G., and D. A. Weitz. 1995. Optical measurements of the linear viscoelastic moduli of complex fluids. *Phys. Rev. Lett.* 74:318–321.

Meechai, N., A. M. Jamieson, and J. Blackwell. 1999. Translational diffusion coefficients of bovine serum albumin in aqueous solution at high ionic strength. *J. Coll. Int. Sci.* 218:167–175.

Morse, D. C. 1998. Viscoelasticity of concentrated isotropic solutions of semiflexible polymers. II. Linear response. *Macromolecules.* 31: 7044–7067.

Nakata, T., and N. Hirokawa. 1992. Organization of cortical cytoskeleton of cultured chromaffin cells and involvement in secretion as revealed by quick-freeze, deep-etching, and double-label immunoelectron microscopy. *J. Neurosci.* 12:2186–2197.

Palmer, A., J. Xu, S. C. Kuo, and D. Wirtz. 1999. Diffusing wave spectroscopy microrheology of actin filament networks. *Biophys. J.* 76:1063–1071.

Schnurr, B., F. Gittes, F. C. MacKintosh, and C. F. Schmidt. 1997. Determining microscopic viscoelasticity in flexible and semiflexible polymer networks from thermal fluctuations. *Macromolecules.* 30: 7781–7792.

Steyer, J. A., and W. Almers. 1999. Tracking single secretory granules in live chromaffin cells by evanescent-field fluorescence microscopy. *Biophys. J.* 76:2262–2271.

Tang, J. X., P. A. Janmey, T. P. Stossel, and I. Tadanao. 1999. Thiol oxidation of actin produces dimers that enhance the elasticity of the F-actin network. *Biophys. J.* 76:2208–2215.

Wachsstock, D. H., W. H. Schwarz, and T. D. Pollard. 1994. Cross-linker dynamics determine the mechanical properties of actin gels. *Biophys. J.* 66:801–809.

Xu, J., W. H. Schwarz, J. A. Kas, T. P. Stossel, P. A. Janmey, and T. D. Pollard. 1998a. Mechanical properties of actin filament networks depend on preparation, polymerization conditions, and storage of actin monomers. *Biophys. J.* 74:2731–2740.

Xu, J., D. Wirtz, and T. D. Pollard. 1998b. Dynamic cross-linking by α-actinin determines the mechanical properties of actin filament networks. *J. Biol. Chem.* 273:9570–9576.

Yamada, S., D. Wirtz, and S. C. Kuo. 2000. Mechanics of living cells measured by laser tracking microrheology (LTM). *Biophys. J.* 78: 1736–1747.